Hindawi
Advances in Materials Science and Engineering
Volume 2017, Article ID 1893672, 8 pages
https://doi.org/10.1155/2017/1893672

Research Article

Effect of Nickel Content on the Corrosion Resistance of Iron-Nickel Alloys in Concentrated Hydrochloric Acid Pickling Solutions

Nabeel Alharthi,[1,2] El-Sayed M. Sherif,[1,3] Hany S. Abdo,[1,4] and S. Zein El Abedin[3]

[1] *Center of Excellence for Research in Engineering Materials (CEREM), Advanced Manufacturing Institute (AMI), King Saud University, P.O. Box 800, Al-Riyadh 11421, Saudi Arabia*
[2] *Mechanical Engineering Department, King Saud University, P.O. Box 800, Al-Riyadh 11421, Saudi Arabia*
[3] *Electrochemistry and Corrosion Laboratory, Department of Physical Chemistry, National Research Centre, El-Behoth St. 33, Dokki, Cairo 12622, Egypt*
[4] *Mechanical Design and Materials Department, Faculty of Energy Engineering, Aswan University, Aswan 81521, Egypt*

Correspondence should be addressed to El-Sayed M. Sherif; esherif@ksu.edu.sa

Received 23 March 2017; Revised 11 May 2017; Accepted 24 May 2017; Published 22 June 2017

Academic Editor: Simon C. Potter

The effect of Ni content on the resistance against corrosion of Fe-36% Ni and Fe-45% Ni alloys in 1 M hydrochloric acid pickling solution was reported. Various electrochemical and spectroscopic techniques such as potentiodynamic cyclic polarization (CPP), open-circuit potential (OCP), electrochemical impedance spectroscopy (EIS), potentiostatic current-time (PCT), and scanning electron microscopy (SEM), and energy dispersive spectroscopy (EDS) have been employed. CPP measurements indicated that the corrosion current and corrosion rate recorded lower values for the alloy that had higher nickel content. OCP curves proved that the presence of high Ni content shifts the absolute potential to the positive potential direction. EIS results revealed that the surface and polarization resistances were much higher for the alloy with higher Ni content. PCT curves also showed that the absolute currents were lower for Fe-45% Ni alloy. All results were in good agreement with others and confirmed clearly that the corrosion resistance in HCl solutions for Fe-45% Ni alloy was higher than that obtained for Fe-45% Ni alloy.

1. Introduction

Iron-nickel alloys have been widely used in the industry because of its many good characteristics [1–4]. These alloys have unique magnetic properties, good mechanical properties, and low thermal expansion coefficient at lower temperatures. Due to their high corrosion and heat resistances. especially those that have the nickel content in the range of 36% to 46%, they represents one of the most widely used superalloys with a broad variety of applications. For example, Invar alloy (64% Fe-36% Ni) has the lowest expansion of the Fe-Ni alloys [5–8].

It has been reported that the iron-nickel alloys have excellent corrosion resistance in oxidizing solutions [9–12], where the increase of Ni content in the alloy increases its corrosion resistance. Several researchers [10–15] have studied the corrosion and corrosion mitigation of iron-nickel alloys in different aggressive media. Jinlong et al. [10] have reported the corrosion resistance of coarse grained and nanocrystalline Ni-Fe alloys in NaCl solutions and proton exchange membrane fuel cell environment. They found that the coarse grained Ni-Fe alloys possessed higher corrosion resistance than the nanocrystalline alloys and this was due to the more compact passive films formed on the surface of coarse grained Ni-Fe alloys. Raman spectroscopy results indicated that many nanocrystalline boundaries were found in the Ni-Fe alloys that activated the diffusion of nickel, which lead to the formation of more nickel oxides and nickel hydroxides [10]. Gehrmann et al. [12] have investigated the corrosion behavior of different iron-nickel alloys that have between 35 wt% and 82 wt% of nickel in a humidity test between 25°C and 80°C. They found that the presence of higher nickel percent in the

Table 1: Corrosion data obtained from the polarization curves for Fe-36% Ni and Fe-45% Ni in 1 M HCl solutions.

Alloy	Corrosion parameter					
	β_c/V/dec^{-1}	E_{Corr}/V	β_a/Vdec^{-1}	j_{Corr}/μAcm^{-2}	R_p/Ωcm^2	R_{Corr}/mpy
Fe-36% Ni	0.135	−0.475	0.035	55.0	2.197	19.44
Fe-45% Ni	0.100	−0.248	0.048	2.0	70.50	0.728

alloy improves its corrosion resistance [12]. Another study on the corrosion behavior of various iron-nickel alloys in sulfuric acid solution using potentiodynamic polarization technique has also been reported [13]. For iron-nickel alloys containing up to 50% Ni, a preferential dissolution of iron takes place and the percentage of iron controls the dissolution process of the alloy. It has been reported [14] that a top layer of $FeNi_3$ is formed for iron-nickel alloys that have more than 40% iron in the alloy. This was confirmed through studying the electrochemical corrosion behavior of different Fe-Ni alloys starting from 0%, 20%, 40%, 60%, and 80% Ni in sulfuric acid solution [14]. Moreover, the corrosion rate decreases as the content of Ni increases in the alloy.

This work aims at reporting the corrosion behavior of Fe-36% Ni and Fe-45% Ni alloys in concentrated hydrochloric acid (1 M HCl) pickling solutions and understanding the effect of increasing nickel content on the corrosion resistance of the iron-nickel alloys. For the best of our knowledge, the corrosion behavior of these alloys in hydrochloric acid solutions has not been reported in the literature before. The study was carried out using various electrochemical techniques. These methods included the use of potentiodynamic cyclic polarization, open-circuit potential, impedance spectroscopy, and the change of the potentiostatic current with time at 0.150 V (Ag/AgCl). The corroded surfaces of the two nickel alloys after being immersed in 1 M HCl solutions for 96 h were investigated using SEM and EDS. It was expected that the alloy with high nickel content would show better corrosion resistance due to the formation of thicker oxides on the surface of the alloy protects it from being easily corroded.

2. Materials and Methods

Two iron base alloys containing 36% Ni and 45% Ni with less than 1% of Mn + Si + C are named as Fe-36% Ni and Fe-45% Ni alloys, respectively. These alloys have a cylindrical shape with 6.0 mm diameter and were purchased from Goodfellow (Ermine Business Park, Huntingdon, England PE29 6WR). Hydrochloric acid (HCl, 32%) was obtained from Merck and was used as received to prepare 1 M concentration of the acid solution. An electrochemical cell with three-electrode configuration that accommodates for 300 cm^3 was used to perform all electrochemical measurements. The Fe-36% Ni and Fe-45% Ni alloys were used as the working electrodes. A silver/sliver chloride (Ag/AgCl) electrode was employed as the reference electrode. A Pt sheet was the counterelectrode in all electrochemical tests. Only one surface of the iron-nickel electrodes were exposed to the electrolytic solution with 0.6 cm diameter and an area of 0.283 cm^2. The surface of the iron-nickel alloys was polished and ground before being immersed in the electrolytic solutions and performing the electrochemical measurements as reported earlier [14–16].

All electrochemical measurements were performed using an Autolab workstation (Metrohm, Utrecht, Netherlands). The CPP experiments were performed by scanning the potential of the iron-nickel alloys in the hydrochloric acid test solution from −1.200 V in the positive direction to 0.80 V (Ag/AgCl) at a scan rate of 0.003 V/s as has been reported in our previous study [17]. The EIS experiments were carried out at the OCP after immersing the iron-nickel alloys after their immersion in 1 M HCl solutions for 2400 s. The range of the frequency for the EIS was scanned from 100 KHz to 100 mHz using an AC wave of ±5 mV peak-to-peak overlaid on a DC bias potential. The impedance data were collected at a rate of 10 points per decade change in frequency using Powersine software. The change of the chronoamperometric current for the iron-nickel electrodes versus time at 0.150 V versus Ag/AgCl was applied for 3600 s after immersing the tested alloys in 1 M HCl for 2400 s. All electrochemical tests were carried out in triplicate, and good reproducibility was observed. All measurements were carried out on a fresh surface of the alloy with a new portion of the test solution. SEM micrographs and EDS profiles were obtained for the surface of the alloys after 96 hours of immersion in 1 M HCl solutions. For this purpose, we used a scanning electron microscope with an attached energy dispersive spectroscopy (JEOL).

3. Results and Discussion

3.1. CPP Measurements. The cyclic potentiodynamic polarization (CPP) technique is a powerful method to obtain important information about the corrosion parameters of metals and alloys in corrosive media [18–23]. Figure 1 shows the CPP curves obtained for iron (1) Fe-36% Ni and (2) Fe-45% Ni immersed in 1.0 M HCl solutions for 2400 s before measurements. The values of cathodic Tafel (β_c) slope, corrosion potential (E_{Corr}), anodic Tafel (β_a) slope, corrosion current density (j_{Corr}), polarization resistance (R_p), and corrosion rate (R_{Corr}) that were obtained from the CPP curves are depicted in Table 1, where the values of j_{Corr} and E_{Corr} were obtained from the extrapolation of anodic and cathodic Tafel lines located next to the linearized current regions [24–28]. The values of R_p were obtained from the polarization curves using the following equation as reported in the previous studies [24–28]:

$$R_p = \frac{1}{j_{Corr}} \left(\frac{\beta_c \beta_a}{2.3 (\beta_c + \beta_a)} \right). \quad (1)$$

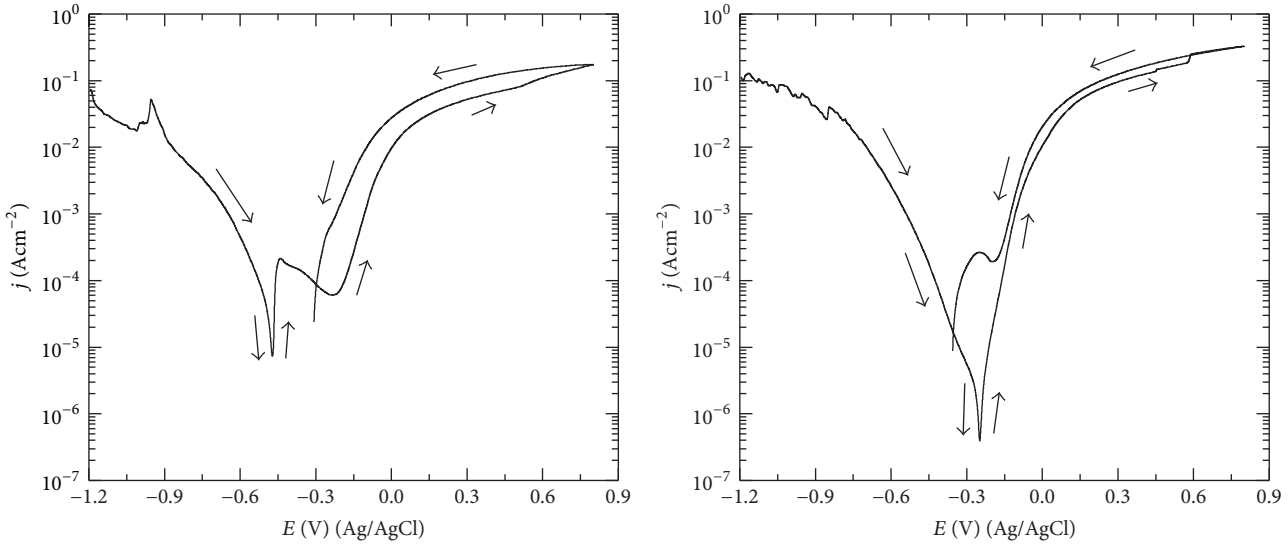

Figure 1: Cyclic potentiodynamic polarization curves obtained for (1) Fe-36% Ni and (2) Fe-45% Ni alloys in 1 M HCl solutions.

Moreover, the values of corrosion rate (R_{Corr}) were obtained as follows [25]:

$$R_{\text{Corr}} = j_{\text{Corr}} \left(\frac{kE_W}{dA} \right). \tag{2}$$

Here, k is a constant, which defines the units for the rate of corrosion (the value of k is 128,800 milli-inches (amp cm year)), E_W is the equivalent weight in grams/equivalent of the tested alloys (the value of E_W is 22.48 for Fe64/Ni36 and 23.44 for Fe55/Ni45), d is the density in gcm^{-3} (8.19 for Fe64/Ni36 and 8.29 for Fe55/Ni45), and A is the area of electrode in cm^2.

It is well known that the cathodic reaction for metals and alloys in concentrated acid solution is the hydrogen evolution reaction, so the cathodic reaction for the nickel alloys in 1 M HCl can be expressed by the following reaction:

$$2H^+ + 2e^- = H_2 \tag{3}$$

While, the anodic reaction at this condition is the dissolution of iron from the surface of the alloy as per the following equation [26];

$$Fe = Fe^{2+} + 2e^- \tag{4}$$

This dissolution reaction explains the abrupt increase of current with increasing the applied potential in the anodic branch. For the anodic side of Fe-36% Ni alloy (Figure 1(a)), the current increased followed by a rapid decrease before abruptly increasing again till the most positive applied potential. The forward anodic side for the second alloy, Fe-45% Ni, shows fast increase of currents with increasing potential without showing any passivation as that recorded for Fe-36% Ni alloy. The first increasing in the current values was due to the dissolution of iron (see (2)), while its decreasing (for Fe-36% Ni alloy) was due to the formation of an oxide film as follows:

$$Fe + \frac{1}{2}O_2 + H_2O = Fe(OH)_2 \tag{5}$$

$$3Fe(OH)_2 + \frac{1}{2}O_2 = Fe_3O_4 + 3H_2O \tag{6}$$

It has been reported [26, 29] that the formation of iron oxide films gives the surface some protection against corrosion. After dissolution of this oxide film, the current increased again till the highest positive value of the applied potential. Moreover, the values of the corrosion parameters listed in Table 1 revealed that the uniform corrosion of Fe-45% Ni alloy in 1 M HCl solution is much lower than its intensity for Fe-36% Ni alloy, where the values of j_{Corr} and R_{Corr} were very low as well as the value of R_P was very high for Fe-45% Ni alloy as can be seen from Table 1. Also, E_{Corr} recorded less negative value for Fe-45% Ni alloy, −0.248 V, while the value of E_{Corr} was more negative for Fe-36% Ni alloy.

Upon reversing the applied potential in the backward direction, the value of the obtained current increases compared to those values obtained in the forward direction for both alloys. It is noted also that the values of current and the hysteresis loop obtained for Fe-36% Ni alloy were much higher than those obtained for Fe-45% Ni alloy. This indicates that the iron-nickel alloys under investigations suffer pitting corrosion and the intensity of pitting is lower for Fe-45% Ni alloy. This was confirmed by the small area of the hysteresis loop obtained for Fe-45% Ni compared to that seen for Fe-36% Ni alloy. The measured CPP results along with the calculated data thus suggested that the alloy with higher nickel content, Fe-45% Ni, has higher resistance against uniform as well as pitting corrosion than the alloy with low

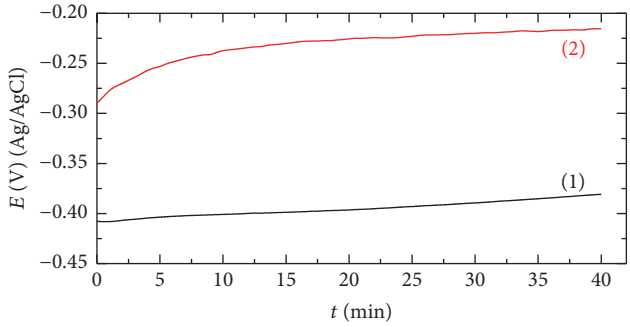

Figure 2: Change of the open-circuit potential with time for (1) Fe-36% Ni and (2) Fe-45% Ni alloys in 1 M HCl solutions.

nickel content, Fe-36% Ni, in 1 M HCl solutions at the same conditions.

3.2. OCP and SEM/EDS Investigations. The change of the free potential, OCP, with time for (1) Fe-36% Ni alloy and (2) Fe-45% Ni alloy in the freely aerated 1 M HCl solutions is depicted in Figure 2. The initial potential of the Fe-36% Ni alloy (curve (1)) recorded almost −0.408 V versus Ag/AgCl and slightly shifted towards the less negative direction with time. The value of OCP for the Fe-36% Ni alloy after 2400 s immersion in the acid solution recorded circa −0.380 V, while the initial potential for the Fe-45% Ni alloy (curve (2)) was almost −0.285 V, which is less negative than that recorded for the Fe-36% Ni alloy. Increasing the immersion time led to further shifts in the less negative direction to record about −0.212 V at the end of the run. The more negative initial potential obtained for Fe-36% Ni alloy is probably due to the corrosivity of the acid solution, which dissolves the surface of the alloy. The shift of potential in the less negative direction resulted from the formation of a thin layer of corrosion products that partially decreases the attack on the surface of the alloy by blocking some of its exposed areas. The positive potential difference between the two alloys is probably due to the higher ability of Fe-45% Ni alloy in developing a thicker layer of corrosion products, which retains a higher corrosion resistance for the Fe-45% Ni alloy compared to Fe-36% Ni alloy.

In order to see the morphology of the surface as well as the elemental analysis for the components on the surface of the alloys after its exposure for long immersion time in the acid test solution, SEM/EDS investigations were carried out. Figure 3 displays (a) SEM micrograph for the surface of the Fe-36% Ni alloy after its immersion in 1 M HCl solutions for 96 h and (b) the corresponding EDS profile analysis shown in the SEM image. Figure 4 also depicts the SEM micrograph (a) and the EDS spectra (b) for the surface of the Fe-45% Ni alloy after its immersion in 1 M HCl solutions for 96 h. It is seen from Figure 3(a) that the surface looks smooth and homogeneous with a thin layer of corrosion products with some deposits. This indicates that the alloy suffers moderate uniform corrosion due to the corrosiveness attack of the acid solution towards the surface without any indications on the occurrence of localized corrosion. The weight percentages (wt.%) of the elements found on the surface were as follows: 49.88 wt.% iron, 39.17 wt.% nickel, 04.89 wt.% oxygen, and 06.06 wt.% carbon. The low percentage of iron and the high percentage detected for nickel compared to its original percentages in the alloy indicate that the dissolution of the alloy took place via the dissolution of Fe as mentioned before in (2). The presence of oxygen also indicates that the corrosion product layer may contain some oxides such as FeO and Fe_2O_3, which may give some protection to the surface of the alloy.

The SEM image shown in Figure 4(a) for the surface of Fe-45% Ni alloy exhibits thicker corrosion product layer compared to the corrosion products shown in Figure 3(a) for Fe-36% Ni alloy. This explains the reason why the potential of Fe-45% Ni alloy shifts towards the positive direction and shows less negative values than those obtained for Fe-36% Ni alloy. The elements found on the surface of the alloy shown in Figure 4(a) and represented by the EDS spectra depicted in Figure 4(b) recorded 26.44 wt.% iron, 14.23 wt.% nickel, 15.38 wt.% oxygen, and 43.94 wt.% chlorine. Here, the very low percentages of iron and nickel compared to their values in the alloy before their exposure to the acid solution are because of the formation of thick layer of corrosion products. This layer fully covers the surface of the alloy leading to its protection and hiding the original surface of the alloy underneath the corrosion products. The high percentages of the detected oxygen confirm that the formed layer on the surface of the alloy has some oxide films. The presence of these oxides increases the passivity of the alloy as well as its corrosion resistance against the harsh effect of the acid solution towards the surface of the alloy. Therefore, it is believed that the formed layer of corrosion products perhaps covers the whole surface of the alloy and decreases the aggressiveness attack of the acid molecules on it and confirms the data obtained by polarization and OCP measurements that Fe-45% Ni alloy has more corrosion resistance compared to the alloy with lower nickel, Fe-36% Ni.

3.3. PCT Measurements. Potentiostatic current-time (PCT) technique has been successfully employed to report the effect of corrosive media on the corrosion, particularly pitting of metals and alloys [14–16, 26]. Here, we used the PCT method to understand the effect of increasing nickel from 36% to 45% on the corrosion of the tested iron-nickel alloys in 1.0 M hydrochloric acid pickling solution. Figure 5 depicts the current-time behavior of (1) Fe-36% Ni and (2) Fe-45% Ni alloys after their immersion in the acid solutions for 2400 s before stepping the potential to 0.150 V versus Ag/AgCl. The current that was recorded for Fe64/Ni36 alloy, Figure 5 (curve (1)), showed abrupt increase from ~88 mA/cm^2 upon the application of the potential to circa 98 mA/cm^2 in the first 200 seconds. This increase of current has resulted from a partial dissolution of the corrosion product layer that might have formed on the surface during the immersion of the alloy before applying the anodic potential. Prolonging the time of the applied potential after the first 200 seconds and till the end of the run has resulted in rapid and continuous decreasing in the current values. This is perhaps due to the thickening of a formed layer of corrosion products on the surface of the

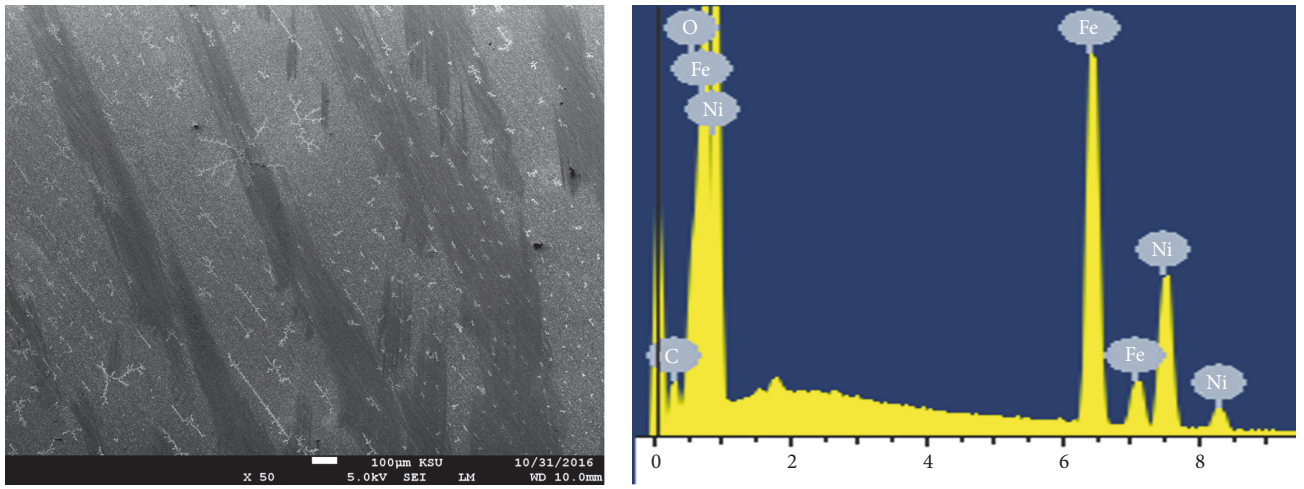

(a) (b)

Figure 3: (a) SEM micrograph for the surface of the Fe-36% Ni alloy after its immersion in 1 M HCl solutions for 96 h and (b) the corresponding EDS profile analysis shown in the SEM image.

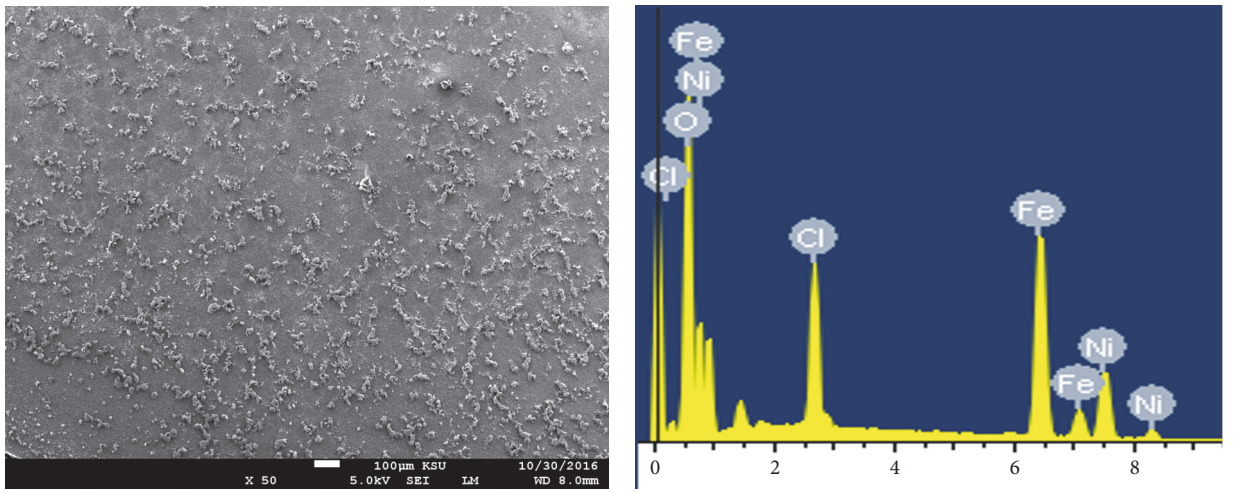

(a) (b)

Figure 4: (a) SEM micrograph for the surface of the Fe-45% Ni alloy after its immersion in 1 M HCl solutions for 96 h and (b) the corresponding EDS profile analysis shown in the SEM image.

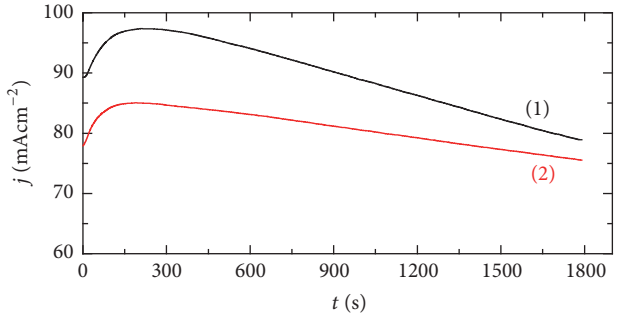

Figure 5: Chronoamperometric curves obtained for (1) Fe-36% Ni and (2) Fe-45% Ni immersed in 1 M HCl solutions for 2400 s followed by stepping the potential to +0.150 V versus Ag/AgCl.

alloy, which protects the surface from being attacked by the aggressiveness action of the acid solutions.

On the other hand, the initial current recorded lower value (~77 mA/cm^2) for Fe-45% Ni alloy that value increases in the first 150 seconds to circa 85 mA/cm^2. The current then decreased with the increase of time till the end of the experiment. Here, the initial increase of current is due to the sudden application of the active potential as well as the dissolution of some of the corrosion products, which were formed during the immersion of the alloy in the solution before applying the potential, while the continuous decrease of current with time was due to the ability of the nickel alloy to develop a protective layer that has iron oxides; this layer

Table 2: Electrochemical impedance spectroscopy parameters obtained for Fe-36% Ni and Fe-45% Ni alloys after their immersions in 1 M HCl solutions.

Alloy	EIS parameter						
	R_S/Ω	Q1		R_{P1}/Ω	Q2		R_{P2}/Ω
		Y_{Q1}/F	n_1		Y_{Q1}/F	n_2	
Fe-36% Ni	2.71	0.06414	0.88	76.6	0.002859	0.81	1166
Fe-45% Ni	3.54	0.02633	1.0	270.9	0.002612	0.94	1385

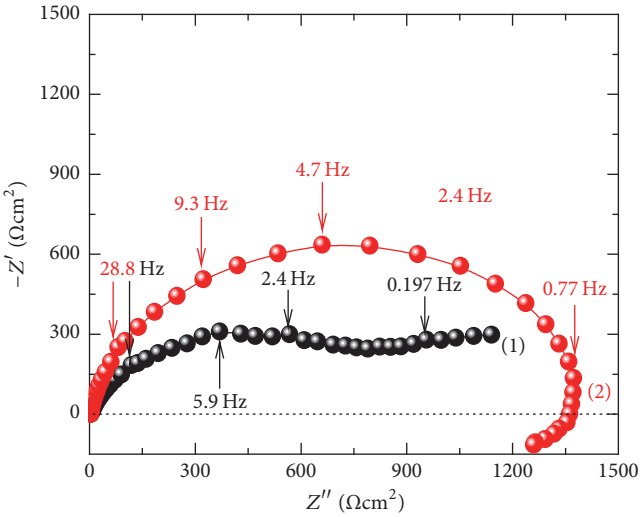

Figure 6: Nyquist plots obtained for (1) Fe-36% Ni and (2) Fe-45% Ni alloys in after their immersion for 2400 s in 1 M HCl pickling solutions.

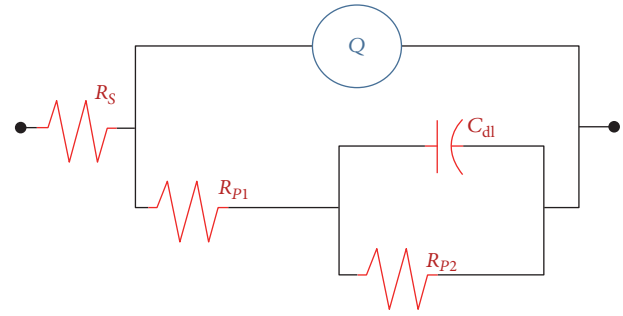

Figure 7: The equivalent circuit model used to fit EIS data shown in Figure 6.

isolates the surface from being in real contact with the acid solution and thus prevents its corrosion. It is seen, thus, that the absolute currents recorded for Fe-45% Ni alloy are lower than those values obtained for Fe-36% Ni alloy over the whole time of the experiment, which reveals that Fe-45% Ni alloy shows more corrosion resistance than Fe-36% Ni one when exposed to the acid solution. Moreover, the change of current with time for these alloys confirms that these materials do not suffer pitting corrosion at this condition.

3.4. EIS Measurements. Electrochemical impedance spectroscopy (EIS) investigations have been widely used to report the kinetic parameters for the electron transfer at the materials/solution interface [26–30]. We have successfully employed this method to investigate the corrosion and corrosion protection of different metals and alloys in various corrosive media [26–33]. Typical Nyquist plots obtained for iron/nickel alloys, (a) Fe-36% Ni and (b) Fe-45% Ni after their immersion for 40 in 1 M HCl, are shown in Figure 6. The Nyquist plot obtained for Fe-36% Ni alloy shows one small semicircle followed by a short segment. And the Fe-45% Ni alloy depicted only one wider semicircle with higher values of both real and imaginary resistances. The smaller diameter of the semicircle obtained for Fe-36% Ni alloy indicates that the alloy has low corrosion resistance as a result of the chloride ions attack. The appearance of the segment following the semicircle reveals that the surface forms a corrosion product layer that protects the surface from further dissolution. It is generally believed that the wider the diameter of the semicircle, the higher the corrosion resistance of the alloy. The wider diameter obtained for the Fe-45% Ni alloy confirms that this alloy has higher corrosion resistance than that for Fe-36% Ni alloy.

For further studying the effect of the acid solution on the iron-nickel alloys, the obtained EIS data were best simulated to an equivalent circuit model and the schematic diagram for that circuit is displayed in Figure 7. The elements depicted in Figure 7 can be defined as follows: R_S refers to the resistance of the solution, Q_1 (Y_{Q1}, CPEs) represents the first constant phase elements at the interface between the nickel alloy and solution, R_{p1} is the polarization resistance at the electrode/solution interface, Q_2 (Y_{Q2}, CPEs) represents another constant phase elements at the interface between a corrosion product layer formed on the alloy's surface and the solution, and R_{p2} is the polarization resistance between the corrosion product layer formed on the alloy and the solution interface and can also be defined as the charge transfer resistance.

The values for the elements of the equivalent circuit that is presented in Figure 7 are listed in Table 2. The data shown in Figure 6 and the parameters listed in Table 2 confirm that the corrosion resistance of Fe-45% Ni alloy is too high compared to that obtained for Fe-36% Ni alloy. This is because the values of R_S, R_{p1}, and R_{p2} for Fe-45% Ni alloy are much higher. It is worth mentioning also that the values of the CPEs (Q_1 and Q_2) with their n_1 and n_2 components were close to unity (exactly ranged from 0.81 to 1.0) and are considered as double layer capacitors [29–31]. Thus, obtained values of Y_{Q1} and Y_{Q2} in the case of Fe-45% Ni alloy are smaller than the values recorded for the Fe-36% Ni alloy.

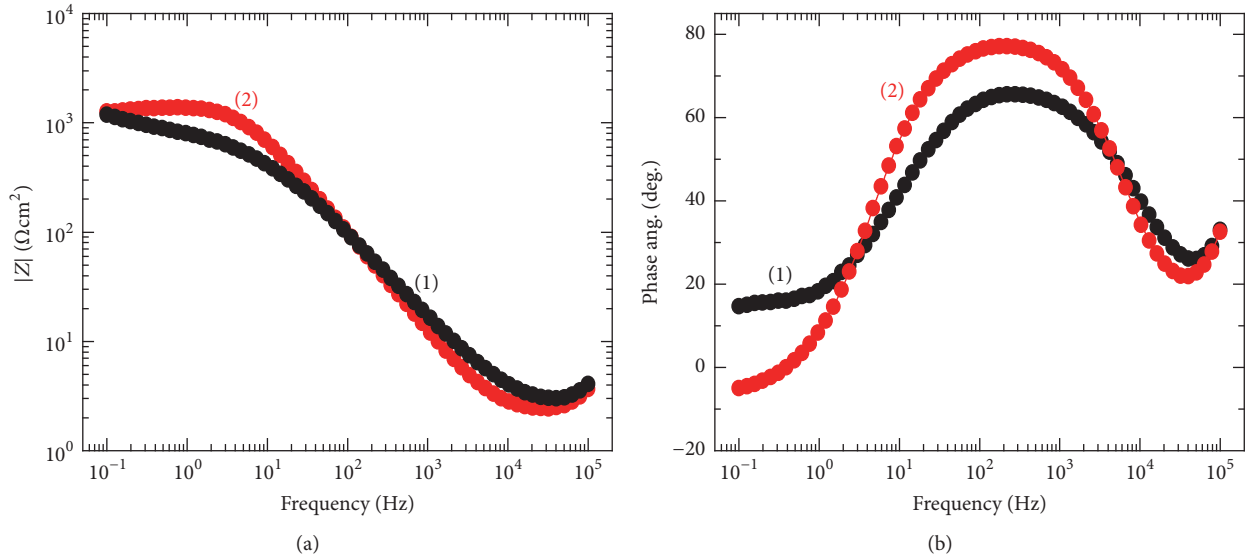

FIGURE 8: Typical Bode: (a) impedance of the interface, $|Z|$, and (b) phase angle plots obtained for iron-nickel alloy: (1) Fe-36% Ni and (2) Fe-45% Ni immersed in 1 M HCl solutions.

In order to throw more light on the dissolution of the two nickel alloys and to further understand the role of increasing Ni content in this process, the Bode impedance of the interface, $|Z|$, and Bode degree of phase angle, (Φ), plots obtained for (1) Fe-36% Ni alloy and (2) Fe-45% Ni alloy immersed in HCl solutions for 2400 s are shown in Figures 8(a) and 8(b), respectively. It is seen from Figure 8(a) that the value of $|Z|$ increases from the higher frequency region towards the low frequency region for the two nickel alloys but with higher $|Z|$ values obtained for Fe-45% Ni alloy (curve (2)), particularly at the low frequency area, compared to Fe-36% Ni alloy. Furthermore, Figure 8(b) depicts that the maximum values recorded for Φ were obtained for Fe-45% Ni alloy (curve (2)). It is generally believed that the high values of $|Z|$ at the low frequency regions as well as the increase of the maximum values of Φ indicate the high corrosion resistance of the material and thus the corrosion resistance for Fe-45% Ni alloy is higher than Fe-36% Ni alloy. The impedance data thus prove that the increase of Ni content increases the corrosion resistance of the iron-nickel alloys. The EIS results thus agree with the data obtained by polarization, OCP, and chronoamperometric current-time measurements that Fe-45% Ni alloy resists corrosion in 1 M HCl solutions more than Fe-36% Ni alloy.

4. Conclusions

The corrosion resistance of Fe-36% Ni alloy and Fe-45% Ni alloy in 1 M HCl solutions was investigated using different electrochemical and spectroscopic techniques. The parameters extracted from polarization curves indicated that the values of j_{Corr} and R_{Corr} were low, while the value of R_p was high for Fe-45% Ni alloy compared to those values obtained for Fe-36% Ni alloy. A potential difference of circa 0.18 V (Ag/AgCl) in the less negative direction was recorded for Fe-45% Ni alloy as indicated by OCP measurement. SEM/EDS investigations after 96 h in the acid test solution showed that the surface of Fe-45% Ni alloy developed a thicker corrosion product layer. EIS data revealed that the diameter of the semicircle of the Nyquist plots was wider and also the values of surface and polarization resistances were higher for Fe-45% Ni alloy than those recorded for Fe-36% Ni alloy. The current-time measurements confirmed that the absolute current values obtained for Fe-36% Ni alloy at 0.150 V (Ag/AgCl) were higher as compared to the values obtained for Fe-45% Ni alloy. Results together were consistent with each other confirming that Fe-45% Ni alloy showed much better corrosion resistance than Fe-36% Ni alloy in 1 M HCl solutions.

Conflicts of Interest

The authors declare that there are no conflicts of interest regarding the publication of this paper.

Acknowledgments

The authors would like to extend their sincere appreciation to the Deanship of Scientific Research at King Saud University for its funding of this research through the Research Group Project no. RGP-160.

References

[1] O. Yamada, I. Nakai, H. Fujiwara, and F. Ono, "High-field susceptibility and magnetization in Fe-Ni invar alloys," *Journal of Magnetism and Magnetic Materials*, vol. 10, no. 2-3, pp. 155-156, 1979.

[2] O. Yamada, F. Ono, and I. Nakai, "The Arrott plots and the itinerant electron character for Fe-Ni invar alloys," *Physica B+C*, vol. 91, pp. 298–301, 1977.

[3] E. P. Wohlfarth, "Invar behaviour in crystalline and amorphous alloys," *Journal of Magnetism and Magnetic Materials*, vol. 10, no. 2-3, pp. 120–125, 1979.

[4] D. Jiles, *Introduction to Magnetism and Magnetic Materials*, Chapman & Hall, London, UK, 1994.

[5] Z.-K. Liu, Y. Wang, and S. Shang, "Thermal expansion anomaly regulated by entropy," *Scientific Reports*, vol. 4, p. 7043, 2014.

[6] C. Woolger, "Invar nickel-iron alloy: 100 years on," *Materials World*, vol. 4, no. 6, pp. 332-333, 1996.

[7] S.-H. Kim, H.-J. Sohn, Y.-C. Joo et al., "Effect of saccharin addition on the microstructure of electrodeposited Fe-36 wt.% Ni alloy," *Surface and Coatings Technology*, vol. 199, no. 1, pp. 43–48, 2005.

[8] L. L. Hamer, "Invar at 100 years," *Advanced Materials and Processes*, vol. 151, pp. 31–34, 1997.

[9] Y. Ihara, H. Ohgame, K. Sakiyama, and K. Hashimoto, "The corrosion behaviour of nickel in hydrogen chloride gas and gas mixtures of hydrogen chloride and oxygen at high temperatures," *Corrosion Science*, vol. 22, no. 10, pp. 901–912, 1982.

[10] L. Jinlong, L. Tongxiang, and W. Chen, "Comparison of corrosion behavior between coarse grained and nanocrystalline Ni-Fe alloys in chloride solutions and proton exchange membrane fuel cell environment by EIS, XPS and Raman spectra techniques," *Energy*, vol. 112, pp. 67–74, 2016.

[11] H. Konishi, M. Yamashita, H. Uchida, and J. Mizuki, "Characterization of rust layer formed on Fe, Fe-Ni and Fe-Cr alloys exposed to Cl-rich environment by Cl and Fe K-Edge XANES measurements," *Materials Transactions*, vol. 46, no. 2, pp. 329–336, 2005.

[12] B. Gehrmann, H. Hattendorf, A. Kolb-Telieps, W. Kramer, and W. Möttgen, "Corrosion behaviour of softmagnetic iron-nickel alloys," *Materials and Corrosion*, vol. 48, no. 8, pp. 535–541, 1997.

[13] D. O. Condit, "Potentiodynamic polarization studies of Fe-Ni binary alloys in sulfuric acid solution at 25°C," *Corrosion Science*, vol. 12, no. 5, pp. 451–462, 1972.

[14] E.-S. M. Sherif, J. A. Mohammed, H. S. Abdo, and A. A. Almajid, "Corrosion behavior in highly concentrated sodium chloride solutions of nanocrystalline aluminum processed by high energy ball mill," *International Journal of Electrochemical Science*, vol. 11, no. 2, pp. 1355–1369, 2016.

[15] E.-S. M. Sherif, H. S. Abdo, J. A. Mohammed, A. A. Almajid, and A. H. Seikh, "Corrosion of newly manufactured nanocrystalline Al and two of its alloys in stagnant 4.0% NaCl solutions," *International Journal of Electrochemical Science*, vol. 11, no. 6, pp. 4598–4610, 2016.

[16] E.-S. M. Sherif, H. S. Abdo, K. A. Khalil, and A. M. Nabawy, "Effect of titanium carbide content on the corrosion behavior of Al-TiC composites processed by high energy ball mill," *International Journal of Electrochemical Science*, vol. 11, no. 6, pp. 4632–4644, 2016.

[17] A. AlOtaibi, E.-S. M. Sherif, S. Zinelis, and Y. S. Al Jabbari, "Corrosion behavior of two cp titanium dental implants connected by cobalt chromium metal superstructure in artificial saliva and the influence of immersion time," *International Journal of Electrochemical Science*, vol. 11, no. 7, pp. 5877–5890, 2016.

[18] M. A. Amin, H. H. Hassan, and S. S. Abd El Rehim, "On the role of NO_2^- ions in passivity breakdown of Zn in deaerated neutral sodium nitrite solutions and the effect of some inorganic inhibitors. Potentiodynamic polarization, cyclic voltammetry, SEM and EDX studies," *Electrochimica Acta*, vol. 53, no. 5, pp. 2600–2609, 2008.

[19] A. Shahryari, W. Kamal, and S. Omanovic, "The effect of surface roughness on the efficiency of the cyclic potentiodynamic passivation (CPP) method in the improvement of general and pitting corrosion resistance of 316LVM stainless steel," *Materials Letters*, vol. 62, no. 23, pp. 3906–3909, 2008.

[20] Z. Bou-Saleh, A. Shahryari, and S. Omanovic, "Enhancement of corrosion resistance of a biomedical grade 316LVM stainless steel by potentiodynamic cyclic polarization," *Thin Solid Films*, vol. 515, no. 11, pp. 4727–4737, 2007.

[21] E.-S. M. Sherif and A. A. Almajid, "Anodic dissolution of API X70 pipeline steel in Arabian Gulf seawater after different exposure intervals," *Journal of Chemistry*, vol. 2014, Article ID 753041, 7 pages, 2014.

[22] M. Saremi and E. Mahallati, "A study on chloride-induced depassivation of mild steel in simulated concrete pore solution," *Cement and Concrete Research*, vol. 32, no. 12, pp. 1915–1921, 2002.

[23] H. Liu, Y. X. Leng, G. Wan, and N. Huang, "Corrosion susceptibility investigation of Ti-O film modified cobalt-chromium alloy (L-605) vascular stents by cyclic potentiodynamic polarization measurement," *Surface and Coatings Technology*, vol. 206, no. 5, pp. 893–896, 2011.

[24] V. Shinde and P. P. Patil, "Evaluation of corrosion protection performance of poly(o-ethyl aniline) coated copper by electrochemical impedance spectroscopy," *Materials Science and Engineering B*, vol. 168, no. 1, pp. 142–150, 2010.

[25] E.-S. M. Sherif, H. S. Abdo, K. A. Khalil, and A. M. Nabawy, "Corrosion properties in sodium chloride solutions of Al–TiC composites in situ synthesized by HFIHF," *Metals*, vol. 5, no. 4, pp. 1799–1811, 2015.

[26] E.-S. M. Sherif, R. M. Erasmus, and J. D. Comins, "In situ Raman spectroscopy and electrochemical techniques for studying corrosion and corrosion inhibition of iron in sodium chloride solutions," *Electrochimica Acta*, vol. 55, no. 11, pp. 3657–3663, 2010.

[27] E.-S. M. Sherif, A. T. Abbas, D. Gopi, and A. M. El-Shamy, "Corrosion and corrosion inhibition of high strength low alloy steel in 2.0 M sulfuric acid solutions by 3-Amino-1,2,3-triazole as a corrosion inhibitor," *Journal of Chemistry*, vol. 2014, Article ID 538794, 8 pages, 2014.

[28] F. H. Latief, E.-S. M. Sherif, A. A. Almajid, and H. Junaedi, "Fabrication of exfoliated graphite nanoplatelets-reinforced aluminum composites and evaluating their mechanical properties and corrosion behavior," *Journal of Analytical and Applied Pyrolysis*, vol. 92, no. 2, pp. 485–492, 2011.

[29] A.-C. Ciubotariu, L. Benea, M. Lakatos-Varsanyi, and V. Dragan, "Electrochemical impedance spectroscopy and corrosion behaviour of Al_2O_3-Ni nano composite coatings," *Electrochimica Acta*, vol. 53, no. 13, pp. 4557–4563, 2008.

[30] M. Kendig and J. Scully, "Basic aspects of electrochemical impedance application for the life prediction of organic coatings on metals," *Corrosion*, vol. 46, no. 1, pp. 22–29, 1990.

[31] F. L. Floyd, S. Avudaiappan, J. Gibson et al., "Using electrochemical impedance spectroscopy to predict the corrosion resistance of unexposed coated metal panels," *Progress in Organic Coatings*, vol. 66, no. 1, pp. 8–34, 2009.

[32] Y. S. Huang, X. T. Zeng, X. F. Hu, and F. M. Liu, "Corrosion resistance properties of electroless nickel composite coatings," *Electrochimica Acta*, vol. 49, no. 25, pp. 4313–4319, 2004.

[33] C. Cao, "On electrochemical techniques for interface inhibitor research," *Corrosion Science*, vol. 38, no. 12, pp. 2073–2082, 1996.